

# Synthesis of Zeolite Na-LSX from Iraqi Natural Kaolin Using Alkaline Fusion before Hydrothermal Synthesis Technique

Ali Mohammed Salih<sup>1</sup>, Craig Williams<sup>2</sup>, Polla Khanaqa<sup>1</sup>

<sup>1</sup>Department of Geology, Kurdistan Institution for Strategic Studies and Scientific Research, Sulaimani, Kurdistan Region - F.R. Iraq

<sup>2</sup>Department of Chemistry and Forensic Science, School of Biology, Faculty of Science and Engineering, University of Wolverhampton, United Kingdom

\*Corresponding author's email: shwangeology@yahoo.com

Received: 09 December 2019

Accepted: 31 January 2019

Available online: 12 March 2019

## ABSTRACT

The synthesis of zeolite materials by hydrothermal transformation of kaolin using an alkaline fusion prior to hydrothermal synthesis method was investigated. The kaolin clay used in the present investigation was supplied from Iraq. The physical and chemical characterization of the starting kaolin and produced zeolite Na-LSX samples were carried out using different analytical techniques such as Scanning Electron Microscopy (SEM), Energy Dispersive Spectroscopy (EDS), X-Ray Diffraction (XRD), X-Ray Fluorescence (XRF), Thermogravimetric Analysis (TGA), Fourier Transform Infrared (FT-IR) Spectroscopy and Inductively Coupled Plasma-Optical Emission Spectrometer (ICP-OES). An alkaline fusion method was introduced prior to the hydrothermal treatment while kaolin powder was mixed manually with NaOH (ratio = 1/1.2 in weight). The metakaolinisation phase was achieved by calcining the mixture in air at 600 oC for 1hr. The result from this route shows that zeolite Na-LSX with cubic rounded edge crystal habit have been successfully synthesised. Finally, The kinetic study indicated the suitability of the zeolite Na-LSX for the removal of Cu<sup>2+</sup>, Fe<sup>3+</sup>, Pb<sup>2+</sup> and Zn<sup>2+</sup> ions from synthetic wastewater.

**Keywords:** Adsorption, Hydrothermal synthesis, Kaolin, Metakaolin, Natural Zeolite, Synthetic Zeolite, Waste water

## 1. INTRODUCTION

A base material that contains a high level of silica and alumina can be used for the preparation of synthetic zeolites such as clay minerals, volcanic glasses, diatomite, natural zeolites, high silica bauxite, or oil shale.

With regard to the use of kaolin as a precursor for zeolite production, the previous studies have shown that an improvement in the properties of the kaolin using chemical methods, which is necessary for zeolite formation but is

difficult due to its low reactivity (Kovo and Holmes, 2010; Petrov and Michalev, 2012; Adamczyk and Bialecka, 2005; Querol *et al.*, 1997; Saija *et al.*, 1983). The previous experiments have established that the preparation of synthetic zeolites from chemical sources of silica and alumina can be expensive, while the conversion of raw materials (natural sources of silica and alumina) into zeolitic materials synthesized by hydrothermal transformation is much cheaper (Tanaka *et al.*, 2004; Ayele *et al.*, 2015; Walek *et al.*, 2008; Wang *et al.*, 2008).

Kaolin does not show significant change by acid or alkaline treatments only (Lussier, 1991). Therefore, kaolin needs to be decomposed by calcination at temperatures between 550 and 950°C to obtain a metakaolin phase after the loss of structural water and reorganization of the structure (Lambert *et al.*, 1989; Mackenzie, 1971). The transition of kaolin, when heated in a furnace in which air is circulating, has been reported and found that metakaolinization achieved

### Access this article online

DOI: 10.25079/ukhjse.v3n1y2019.pp10-17 E-ISSN: 2520-7792

Copyright © 2019 Salih, *et al.* Open Access journal with Creative Commons Attribution Non-Commercial No Derivatives License 4.0 (CC BY-NC-ND 4.0).

by calcining the kaolin in open air at around 550–900°C with different exposure times (Breck, 1974; Madani *et al.*, 1989; Brindley and Nakahira, 19859). The previous experiments reported that the best heating values for obtaining a reactive metakaolin can be between 600 and 800°C (Lussier, 1991; Breck, 1974). Mackenzie (1971) showed in his investigation that calcinations of kaolin at very high temperatures resulted in the formation of mullite and cristobalite.

In recent years, there has been much interest in producing synthetic zeolite using low-cost raw materials such as kaolin (natural clays) (Georgiev *et al.*, 2009; Ibrahim *et al.*, 2010; Rondón *et al.*, 2013; Doaa and Mohamed, 2014; Jamil *et al.*, 2010). Nowadays, synthetic zeolites are used commercially more often than natural zeolites due to the homogeneity of their particle sizes and the purity of crystalline products, which result in significantly higher efficiency in heavy metal removal (Szoztak, 1998). Another advantage of synthetic zeolites in comparison to natural zeolites is that synthetic zeolites can be engineered with a wide variety of chemical properties and pore sizes and that they have greater thermal stability (Szoztak, 1998).

Thus, in the present study, Iraqi natural kaolin was used as a starting material to produce zeolite Na-LSX. The zeolite synthesis from Iraqi natural kaolin was carried out using alkaline fusion before hydrothermal synthesis technique.

## 2. EXPERIMENTAL

### 2.1. Raw Materials and Chemical Reagent

In this study, natural zeolite (clinoptilolite) was used. The natural clinoptilolite was mined in Anaconda and supplied by the Anaconda Mining Company, Denver, Colorado, USA; it is 97% pure.

The kaolin clay used in the present investigation was collected from the site in the western part of Iraq and supplied by Kurdistan Institution for Strategic Studies and Scientific Research (KISSR). The natural zeolite and raw material samples were used as received without any modification from their natural state, unless stated. The raw and zeolitic material samples were washed with deionized water to remove unwanted dust from their surfaces before use and then dried at room temperature for about 24 h.

Iraqi row kaolin as an aluminosilicate source was prepared before the synthesis process. Samples were ground manually to powder form in a porcelain mortar and sieved using laboratory soil sieve. The mesh sizes of the kaolin particle selected in this study were  $75 \mu\text{m} < d_p < 125 \mu\text{m}$ .

The synthesis of zeolite Na-LSX from kaolin involves two basic steps: Chemical treatment of raw kaolin using sodium hydroxide (NaOH) applied first, followed by thermal treatment (metakaolinization) of the raw kaolin at high temperature.

An alkaline fusion method was introduced before the hydrothermal treatment as shown in Figure 1. Kaolin powder ( $<125 \mu\text{m}$ ) was mixed manually with NaOH (ratio = 1/1.2 in weight) in a porcelain mortar then the prepared sample was left for 40 min at room temperature.

### 2.2. Hydrothermal Synthesis (Metakaolinization)

Then, the mixture was calcined at 600°C for 1 h to convert Iraqi kaolin to Iraqi metakaolin. The fused solid product obtained had to be ground manually again to powder form in a porcelain mortar.

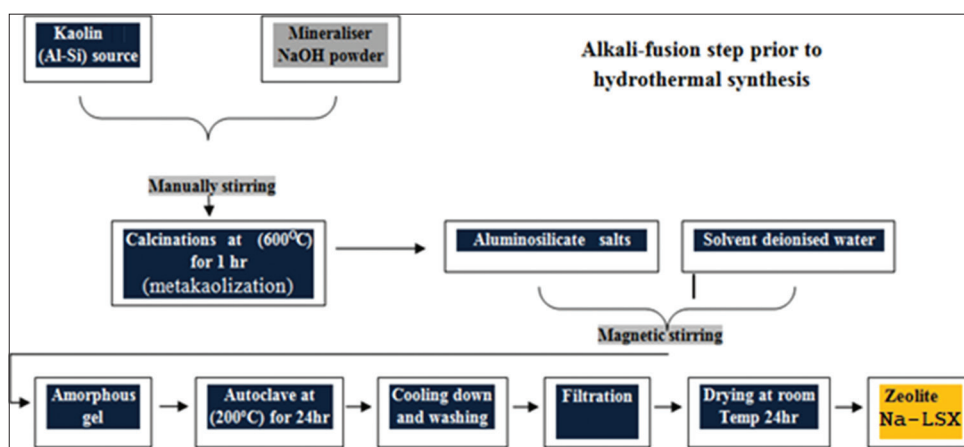


Figure 1. The conversion of the kaolin raw materials into zeolite Na-LSX conducted by alkaline fusion followed by hydrothermal reaction

Then, 5 g of the produced metakaolin was contacted with 25 ml of distilled water (ratio = 1/5) for 15 min at room temperature. The hydrothermal reaction was carried out using stainless steel autoclaves with a Teflon liner heated to 200°C in an oven to insert the sodium ion into the metakaolin. The reactors were removed from the autoclave after 24 h and cooled with water to stop the reaction.

The acid-treated kaolin clay was washed with deionized water 3 times to remove the excess unreacted NaOH. It was then filtered and dried in an oven at 100°C overnight.

During calcination of kaolin, the silicon atoms experience a range of reactions of differing distortion due to dehydroxylation (Bellotto *et al.*, 1995). The aluminum atoms mostly transform from octahedral to tetrahedral geometry. As the calcination temperature increases, the structure becomes more distorted and amorphous silica is then liberated (Bellotto *et al.*, 1995). The dehydroxylation process might result in the disturbance of the Al (O, OH)<sub>6</sub> octahedral sheet by the outer hydroxyls, but it does not have much effect on the SiO<sub>4</sub> tetrahedral sheet due to the more stable inner hydroxyl groups (Rios *et al.*, 2007). The outer hydroxyls of the octahedral sheets may be more easily removed by heating than the inner ones, which will maintain a more ordered SiO<sub>4</sub> tetrahedral group in the structure during dehydroxylation (Rios *et al.*, 2007). After heating at 950°C, the SiO<sub>4</sub> groups combine with the AlO<sub>6</sub> group to form the Al-Si spinel phase, which has a short range order structure (Bellotto *et al.*, 1995).

### 2.3. Characterization of the Untreated and Thermally Treated Kaolin

Knowledge of the characteristics of kaolin, natural zeolite, and synthetic zeolite is very important. The technological properties of kaolin and zeolite products depend on the physical, chemical, and mineralogical characteristics of the starting materials; this also controls the overall processing treatment of polluted effluents.

The study of characterization of the zeolite is to provide information on (a) its structure and morphology; (b) its chemical composition; (c) its ability to sorb and retain molecules; and (d) its ability to chemically convert those molecules.

Thus, different analytical techniques were used to study kaolin and both natural and synthesis zeolite product samples. This used analytical techniques including scanning electron microscopy (SEM), energy-dispersive spectroscopy (EDS), X-ray diffraction (XRD), X-ray fluorescence (XRF), thermogravimetric analysis (TGA), Fourier transform

infrared (FT-IR), and inductively coupled plasma-optical emission spectrometers (ICP-OES).

## 3. BATCH ADSORPTION STUDIES

Batch studies were used to investigate the behavior of both natural zeolite and synthetic zeolite Na-LSX and to understand the metal removal efficiency from solution. The data obtained from the kinetic adsorption tests were used to determine the percentage removal of metal ions from solution were also determined using the equation below:

$$\text{Percentage adsorbed (\% removal)} q_e = \{(C_o - C_e) - 100\} / C_o$$

Where,

$q_e$  is the amount of adsorbate adsorbed per unit weight of adsorbent (mg/g)

$C_o$  and  $C_e$  are the initial and final metal ion concentrations in solution (mg/l), respectively,  $V$  is the solution volume (l) and  $m$  is the weight of the zeolite used (g).

All natural and synthetic zeolite samples with masses 4 g were contacted with constant volume (100 ml) of multicomponent synthetic solutions containing Cu<sup>2+</sup>, Fe<sup>3+</sup>, Co<sup>2+</sup>, and Zn<sup>2+</sup> ions. They were agitated at agitation speeds of 150 rpm for agitation times of 60, 120, 180, 240, 300, and 360 min in a magnetic stirrer at room temperature. Every hour 15 ml of the samples were filtered and taken for metal ion concentration analysis using the ICP-OES. The pH values were monitored and adjusted regularly.

The experiments were duplicated 3 times to examine the reproducibility of the results, while the mean value was used for all taken data. The deviation between the duplicate samples in analyzing the cations was ± 6.4%, 6.3%, 5.6%, and 6.4% for Cu<sup>2+</sup>, Fe<sup>3+</sup>, Co<sup>2+</sup>, and Zn<sup>2+</sup> ions, respectively.

## 4. RESULTS AND DISCUSSION

### 4.1. SEM Results

The surface morphology, topography of the raw and zeolitic materials, was investigated using a ZEISS EVO50 SEM. The micrographs of the “as received” kaolin samples are represented in Figure 2 and were obtained from SEM analysis under the following SEM analytical conditions: EHT = 20.00 kV, Signal A = VPSE, WD 8.5 mm at a magnification of ×2000 and ×5000. The micrograph of

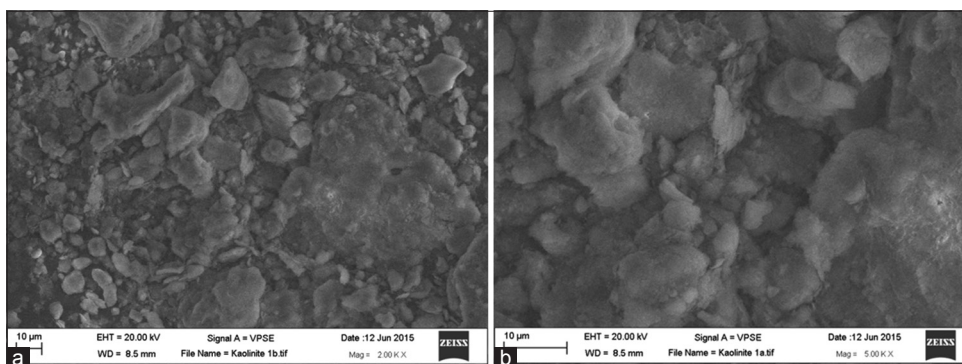


Figure 2. (a and b) SEM micrograph of kaolinite shows the crystalline nature of kaolin at a magnification of  $\times 2000$  and  $\times 5000$

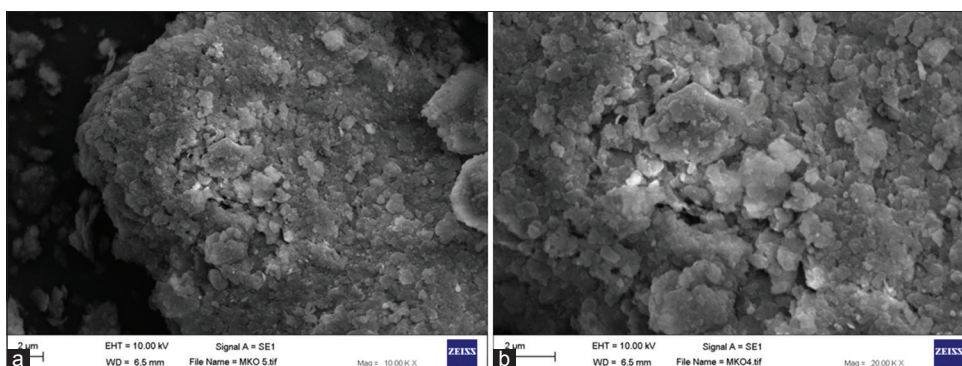


Figure 3. (a and b) SEM micrograph shows the crystalline nature of metakaolin at a magnification of  $\times 10000$  and  $\times 20000$

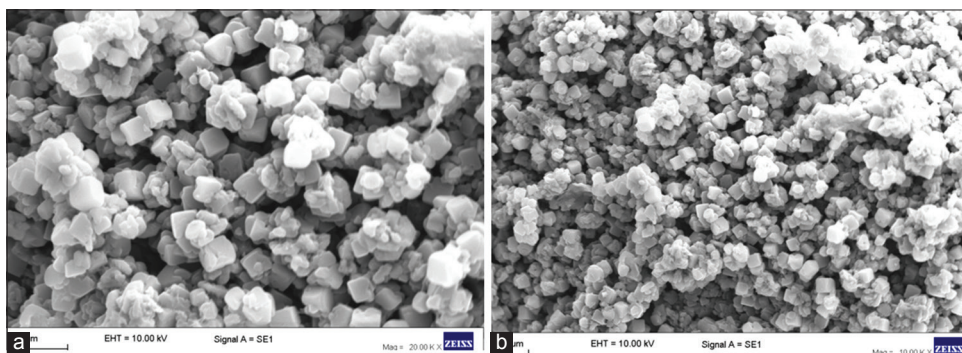


Figure 4. (a and b) SEM microstructure showing the oriented zeolite Na-LSX crystallites synthesized by alkaline fusion followed by hydrothermal reaction

kaolin, which presents crystals of kaolin that is not well defined and randomly oriented crystallites and, in particular, indicates the crystalline nature of Iraqi kaolin before any modification.

The micrographs of the Iraqi metakaolin samples were studied under the following SEM analytical conditions: EHT = 10.00 kV, Signal A = SE1, and WD = 6.5 mm at a magnification of  $\times 20000$  and  $\times 10000$ . The sample was calcined at  $600^{\circ}\text{C}$  for 1 h. The micrographs show the

randomly oriented crystallites and, in particular, indicate the appearance of the partly crystalline (Figure 3).

The micrographs of the synthesized zeolite Na-LSX samples were taken under the following SEM analytical conditions: EHT = 10.00 kV, Signal A = SE1, and WD = 7 mm at magnifications of  $\times 10000$  and  $\times 20000$ . As shown in Figures 4 and 5, the micrograph indicates, in particular, the well-formed typical cubic-shaped crystals of zeolite Na-LSX with an average particle size of  $3.1\ \mu\text{m}$ .

Table 1. The chemical composition (wt. %) of the Iraqi kaolin “as received” used in the preparation of zeolite type A

Element	Na <sub>2</sub> O%	MgO%	Al <sub>2</sub> O <sub>3</sub> %	SiO <sub>2</sub> %	K <sub>2</sub> O%	CaO%	TiO <sub>2</sub> %	Fe <sub>2</sub> O <sub>3</sub> %
EDS	1.64	0.23	13.49	15.72	0.22	0.76	0.70	1.04
XRF	1.74	0.21	30.17	39.37	0.48	0.89	0.78	1.49

EDS: Energy-dispersive spectroscopy, XRF: X-ray fluorescence

Table 2. XRF analysis showing the chemical composition (wt.%) of zeolite A using alkaline fusion before the hydrothermal synthesis route

Element	Na <sub>2</sub> O%	MgO%	Al <sub>2</sub> O <sub>3</sub> %	SiO <sub>2</sub> %	K <sub>2</sub> O%	CaO%	TiO <sub>2</sub> %	Fe <sub>2</sub> O <sub>3</sub> %
XRF	4.877	0.114	14.465	20.731	0.105	0.872	0.67	1.38

XRF: X-ray fluorescence

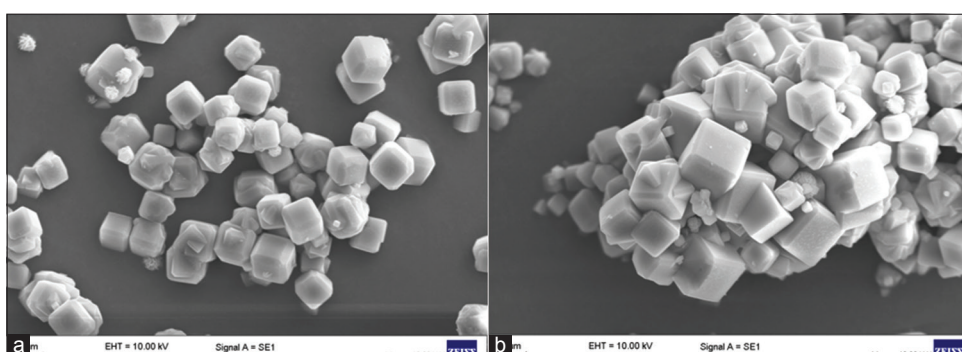
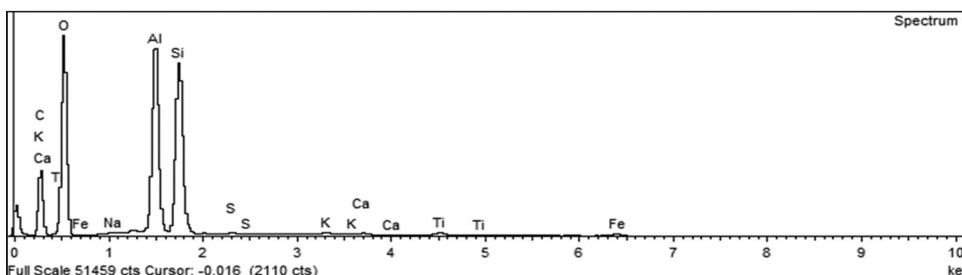
Figure 5. (a and b) SEM microstructure showing the oriented cubic-shaped crystals of zeolite Na-LSX with rounded edges at a magnification of  $\times 10000$ 

Figure 6. Spectral analysis showing the elemental composition for the kaolin sample

#### 4.2. EDS and XRF Results

The EDS (using a ZEISS EVO50 spectrometer) and XRF analysis technique (using the Empyrean, PANalytical XRF spectrometer) were used to determine the chemical composition and elemental analysis of the raw materials and synthesis products. The main chemical composition of Iraqi kaolin and the existence of SiO<sub>2</sub> and AlO<sub>3</sub> in the raw kaolin as an aluminosilicate source used in this study are presented in Table 1. The results of the EDS and XRF analysis show that the predominant exchangeable cations in the kaolin structure were Na<sup>+</sup>, K<sup>+</sup>, Mg<sup>2+</sup>, and Ca<sup>2+</sup> (Figure 6).

The XRF analysis results are showing the chemical composition of Iraqi zeolite-type Na-LSX [Table 2]; these results were obtained after the conversion of the raw materials into zeolitic materials. The results indicate that the major components of zeolite Na-LSX are present in the structure, in addition to trace amounts of impurities associated with the Iraqi raw kaolin used in the preparation, which could not be removed with the preparation procedure used. The predominant exchangeable cations for zeolite Na-LSX were found to be Na<sup>+</sup>, K<sup>+</sup>, Mg<sup>2+</sup>, and Ca<sup>2+</sup>, which verify the results obtained from the EDS analysis.

### 4.3. XRD Analysis

XRD analytical technique used for phase identification of the natural zeolite samples, raw materials, and synthesis products of crystalline materials using the Empyrean, PANalytical X-ray diffractometer. The XRD pattern from synthetic zeolite Na-LSX prepared by alkaline fusion before the hydrothermal synthesis method is shown in Figure 7. Kaolin can be identified by its characteristic XRD peaks. It has peaks at  $12.23^\circ$  and  $24.82^\circ 2\theta$ , which are the characteristic peaks of kaolin as reported the previous studies (Zhao *et al.*, 2004; Gougazeh and Buhl, 2010). The results show that the synthetic zeolites contained major quantities of zeolite Na-LSX with minor quantities of sodalite.

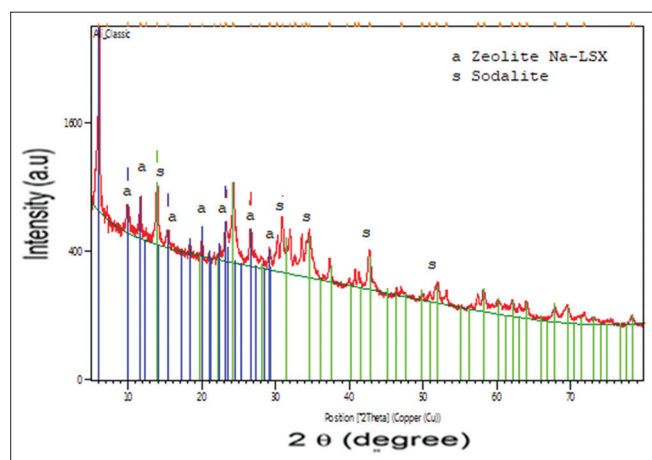


Figure 7. X-ray diffraction (XRD) analysis showing the mineralogical analysis XRD of zeolite Na-LSX

### 4.4. TGA

The TGA technique was used for the measurement of changes in the physical and chemical properties while increasing the temperature constantly. The raw materials were analyzed using thermogravimetry on a Perkin Elmer TGA7 thermobalance between 30 and  $1000^\circ\text{C}$ , using a heating rate of  $20^\circ\text{C min}^{-1}$ . The results from the TGA/DTG show that the zeolite Na-LSX sample underwent continuous weight loss while it was heated to  $900^\circ\text{C}$ . Figure 8 shows obvious weight loss, the main reason is loss in water molecular which appears during dehydration and dehydroxylation process (Murray, 2007). According to Perraki and Orfanoudaki (2004), weight losses at  $<200^\circ\text{C}$  are due to hygroscopic water and loosely bonded water, respectively. Figure 8 shows an endothermic peak at  $160^\circ\text{C}$  due to dehydration. There are another two endothermic peaks, at  $530^\circ\text{C}$  due to dehydroxylation and  $850^\circ\text{C}$  due to the formation of a new solid phase (Sodalite). The total loss calculated from the TGA was 23.5%. However, in this study, a dehydroxylation process occurred between  $450^\circ\text{C}$  and  $600^\circ\text{C}$ .

### 4.5. FT-IR

FT-IR spectra of the raw materials were recorded in the range of  $4000\text{--}400\text{ cm}^{-1}$  using an ALPHA, FTIR with Platinum ATR single reflection diamond module.

A band of weak intensity was observed around  $549\text{ cm}^{-1}$ ; this peak represents the presence of zeolite Na-LSX in the cubic prism form. It could represent the beginning of the

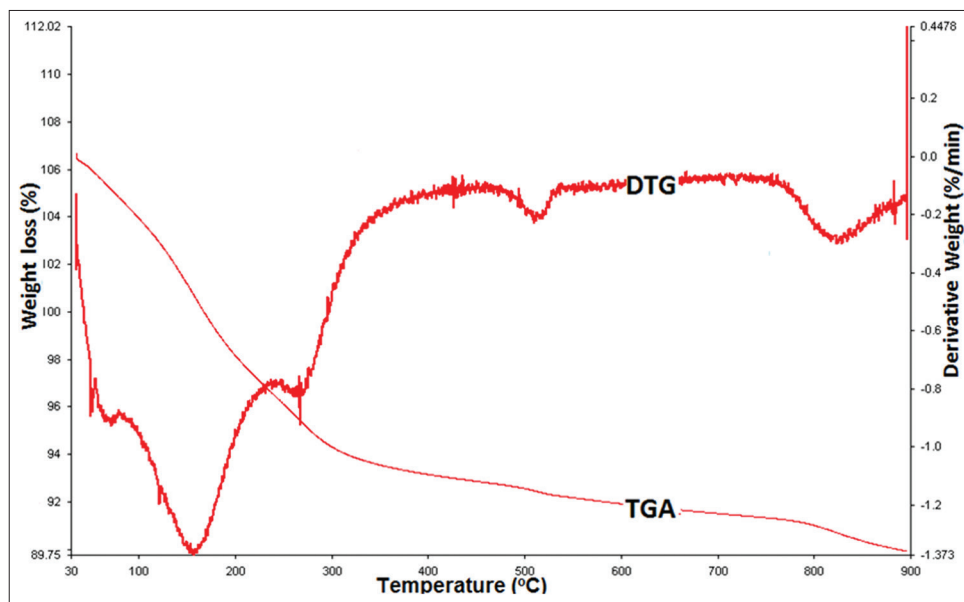


Figure 8. Thermogravimetric analysis (TGA/DTG) of zeolite Na-LSX showing curves between 30 and  $900^\circ\text{C}$

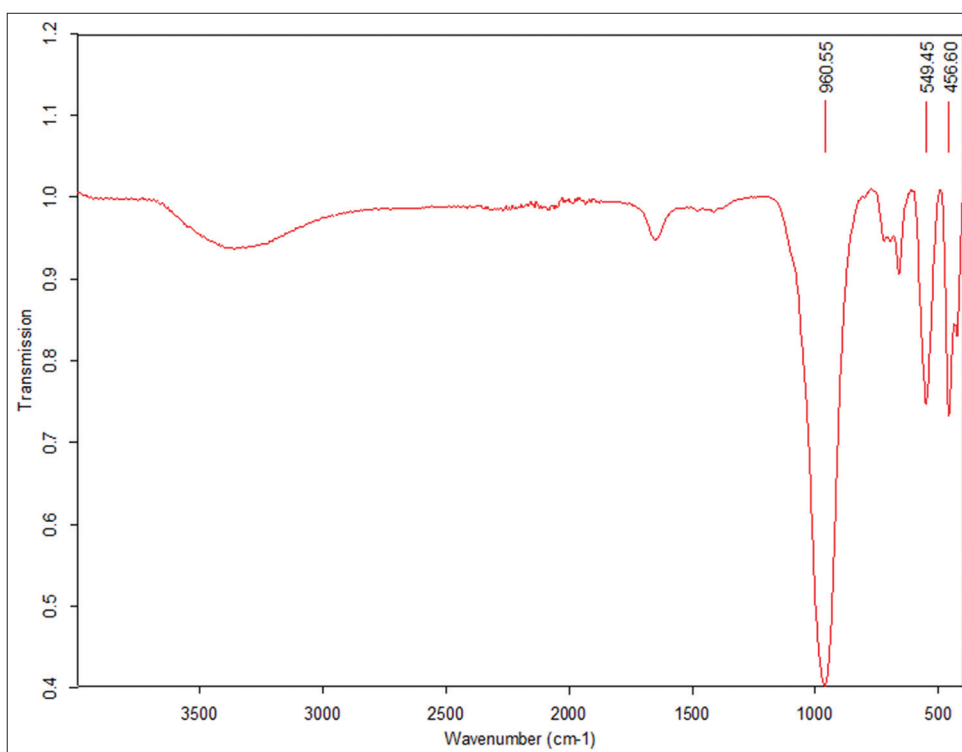


Figure 9. The Fourier transform infrared spectra of zeolite Na-LSX obtained from Iraqi kaolin after treatment

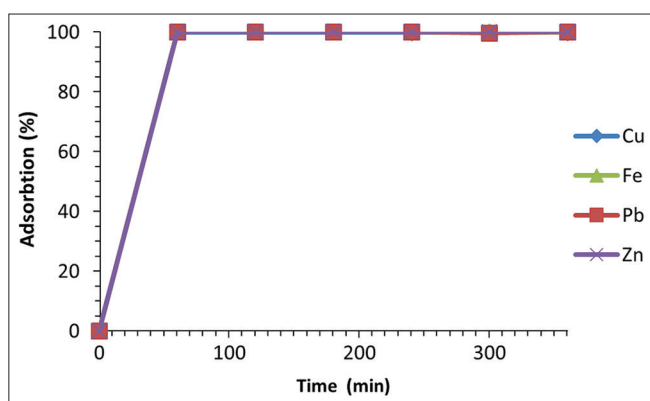


Figure 10. The adsorption of copper, iron, lead, and zinc from solution by zeolite Na-LSX

crystallization of a zeolite with double rings (Alkan *et al.*, 2005). The bands at  $456\text{ cm}^{-1}$  correspond to the internal linkage vibrations of the Si-O-Si or Si-O-Al tetrahedral structure and to the asymmetric stretching, respectively, of zeolite Na-LSX (Alkan *et al.*, 2005). The transformation of Iraqi kaolin to Iraqi zeolite Na-LSX can be clearly observed from FT-IR spectra in the lattice region of  $960\text{--}456\text{ cm}^{-1}$  (Figure 9). The kaolin starting material gives well-defined FT-IR spectra bands in this region due to Si-O, Si-O-Al, and Al-OH vibrations.

#### 4.6. Batch Adsorption Studies

The results show that the uptake of heavy metal cations from solution using synthetic zeolite mostly occurs in the 1<sup>st</sup> h and the highest removal ratio of  $\text{Cu}^{2+}$ ,  $\text{Fe}^{3+}$ ,  $\text{Pb}^{2+}$ , and  $\text{Zn}^{2+}$  ions was achieved > 99 % in the 1<sup>st</sup> h (Figure 10). The percentage adsorbed value of heavy metal cations from solution using natural zeolite passed 90% in the 1<sup>st</sup> h (Figure 11). Hence, the metal removal efficiency from the solution of synthetic zeolite Na-LSX is higher than that of natural zeolite.

## 5. CONCLUSIONS

The following conclusions are based on the results of this investigation:

- The result from alkaline fusion followed by hydrothermal reaction method shows that after both chemical and thermal treatment, zeolite Na-LSX was successfully synthesized.
- From the physicochemical characterization results, it can be generally considered that the kaolin clay used in this study has properties suitable for zeolite Na-LSX synthesis and could be, in principle, a useful source of a cheaper silica and alumina source material. In the meantime, it can reduce material waste.
- Zeolite Na-LSX could be used as a cheap and local

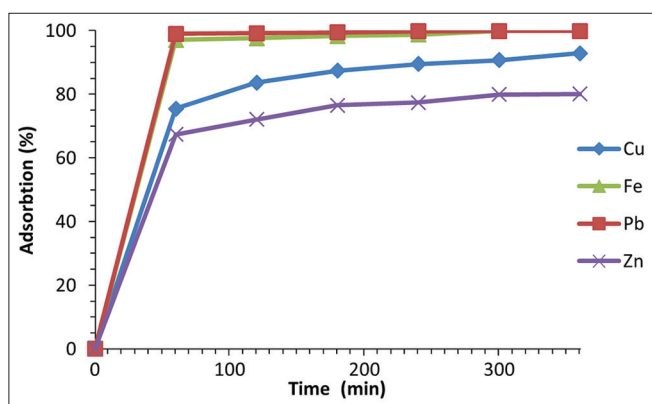


**Figure 11.** The adsorption of copper, iron, lead, and zinc from solution by natural zeolite

adsorbent material for the uptake of heavy metal cations from wastewater. The batch study considered the suitability of the zeolite Na-LSX used for the removal of heavy metal cations from synthetic wastewater.

- The results also showed that the metal removal efficiency of synthetic zeolite Na-LSX from solution is higher than metal removal efficiency of natural zeolite from synthetic wastewater. This is due to continually losing water during dehydroxylation and dehydration process and decomposition of some crystalline structure following by well-defined cubic zeolite crystals.

## REFERENCES

- Adamczyk, Z., & Bialecka, B. (2005). Hydrothermal synthesis of zeolite s from polish coal fly ash. *Polish Journal of Environmental Studies*, 14(6), 713-719.
- Alkan, M., Hopa, C., Yilmaz, Z., & Guler, H. (2005). The effect of alkali concentration and solid/liquid ratio on the hydrothermal synthesis of zeolite NaA from natural kaolin. *Microporous and Mesoporous Materials*, 86, 176-184.
- Ayele, L., Perez-Pariente, J., Chebude, Y., & Diaz, I. (2015). Synthesis of zeolite a from Ethiopian kaolin. *Microporous and Mesoporous Materials*, 215, 29-36.
- Bellotto, M., Gualtieri, A., Artioli, G., & Clark, S. M. (1995). Kinetic study of the kaolinite-mullite reaction sequence. Part I: kaolinite dehydroxylation. *Physics and Chemistry of Minerals*, 22(4), 207-214.
- Breck, D. W. (1974). *Zeolite Molecular Sieves: Structure, Chemistry and Use*. 1<sup>st</sup> ed. New York: John Wiley.
- Brindley, G. W., & Nakahira, M. (1959). The kaolin-mullite reaction series: I, a survey of outstanding problems. *Journal of the American Ceramic Society*, 42, 311-314.
- Doaa, M., & Mohamed, S. (2014). Removal of Pb<sup>2+</sup> from water by using Na-Y zeolite s prepared from Egyptian kaolins collected from different sources. *Journal of Environmental Chemical Engineering*, 2, 723-730.
- Georgiev, D., Bogdanov, B., Angelova, K., Markovska, I., & Hristov, Y. (2009). *Synthetic Zeolites Structure, Classification, Current Trends in Zeolite Synthesis Review*. International Science Conference.
- Stara Zagora, Bulgaria.
- Gougazeh, M., & Buhl, C. H. (2010). Geochemical and mineralogical characterization of the jabal al-harad kaolin deposit, Southern Jordan for its possible utilization clay miner. *Mineralogical Society*, 45(4), 281-294.
- Ibrahim, H. S., Jamil, T., & Eman, Z. H. (2010). Application of zeolite prepared from Egyptian kaolin for the removal of heavy metals: II. Isotherm models. *Journal of Hazardous Materials*, 182, 842-847.
- Jamil, S. T., Ibrahim, H. S., Abd E. I., & El-Wakeel, T. (2010). Application of zeolite prepared from Egyptian kaolin for removal of heavy metals: I. Optimum conditions. *Desalination*, 258, 34-40.
- Kovo, A. S., & Holmes, S. M. (2010). Effect of aging on the synthesis of kaolin-based zeolite Y from Ahoko Nageria using a novel metakaolnization technique. *Journal of Dispersion Science. Technology*, 31, 442-448.
- Lambert, J. F., Minman, W. S., & Fripiat, J. J. (1989). Revisiting kaolin dehydroxylation: A silicon-29 and aluminum-27 MAS NMR study. *Journal of the American Chemical Society*, 111, 3517-3522.
- Lussier, R. (1991). A novel clay-based catalytic material-preparation and properties. *Journal of Catalysis*, 129(1), 225-237.
- Mackenzie, R. C. (1971). Differential thermal analysis 1. *Analytica Chimica Acta*, 53(1), 221.
- Madani, A., Aznar, A., Sanz, J., & Serratos, J. M. (1989). 29Si and 27Al NMR study of zeolite formation from alkali-leached kaolins. Influence of thermal preactivation. *Journal of Physical Chemistry*, 94, 760-765.
- Murray, H. H. (2007). *Applied Clay Mineralogy, Occurrences, Processing and Application of Kaolins, Bentonites, Palygorskite-Sepiolite, and Common Clays*. 1<sup>st</sup> ed. Oxford: Elsevier's Science and Technology.
- Perraki, T., & Orfanoudaki, A. (2004). Mineralogical study of zeolites from Pentafos area. *Applied Clay Science*, 25, 9.
- Petrov, I., & Michalev, T. (2012). Synthesis of zeolite: A review. University of ruse. Union of Scientists Ruse, 51, 30-35. Available from: <http://www.uni-ruse.bg>; <http://www.uni-ruse.bg/suruse>.
- Querol, X., Plana, F., Alastuey, A., & Lopez-Soler, A. (1997). Synthesis of Na-zeolite s from fly ash. *Fuel*, 76, 793-799.
- Rios, C. A., Williams, C. D., & Maple, M. J. (2007). Synthesis of zeolites and zeotypes by hydrothermal transportation of kaolin and metakaolin. *BISTUA*, 5(1), 15-26.
- Rondón, W., Freire, D., Benzo, Z., Sifontes, A., González, Y., Valero, M., & Brito, J. L. (2013). Application of 3A zeolite prepared from Venezuelan kaolin for removal of Pb (II) from wastewater and its determination by flame atomic absorption spectrometry. *American Journal of Analytical Chemistry*, 4, 584-593.
- Saija, L. M., Ottana, R., & Zipelli, C. (1983). Zeolitization of pumice in ash-sodium salt solutions. *Materials Chemistry and Physics*, 8, 207-216.
- Szoztak, R. (1998). *Molecular Sieves: Principles of Synthesis and Identification*. 2<sup>nd</sup> ed. London: Blackie Academic and Professional.
- Tanaka, H., Miyagawa, A., Eguchi, B., & Hino, V. R. (2004). Synthesis of a pure-form Zeolite Na-LSX from coal fly ash by dialysis. *Journal of Industrial and Engineering Chemistry*, 43, 6090-6094.
- Walek, T. T., Saito, F., & Zhang, Q. (2008). The effect of low solid/liquid ratio on hydrothermal synthesis of zeolites from fly ash. *Fuel*, 87, 3194-3199.
- Wang, C. F., Li, J. S., Wang, L. J., & Sun, X. Y. (2008). Influence of NaOH concentrations on synthesis of pure-form zeolite a from fly ash using two-stage method. *Journal of Hazardous Materials*, 155, 58-64.
- Zhao, H., Deng, Y., Harsh, J. B., Flury, M., & Boyle, J. S. (2004). Alteration of kaolin to cancrinite and sodalite by simulated hanford tank waste and its impact on cesium retention. *Clays and Clay Minerals*, 52, 1-13.